

A Scalable Parallel Implementation of Double Porosity/Permeability Model

Mohammad S. Joshaghani, Kalyana B. Nakshatrala

Computational & Applied Mechanics Laboratory
Department of Civil and Environmental Engineering
University of Houston, Texas 77204.

March 12, 2019

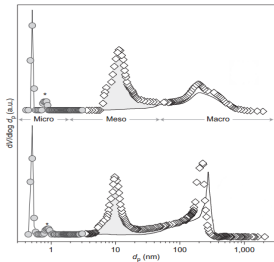
Collaborators: S. H. S. Joodat, J. Chang, and M. G. Knepley

Motivation and insights

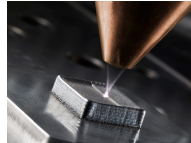
Materials with complex pore-networks



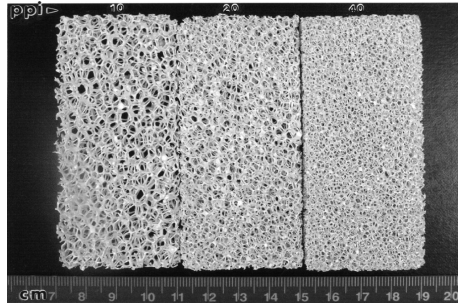
Flow in fissured rocks



[Mitchell et al., *Nature Chemistry*, 4:825-831, 2012]



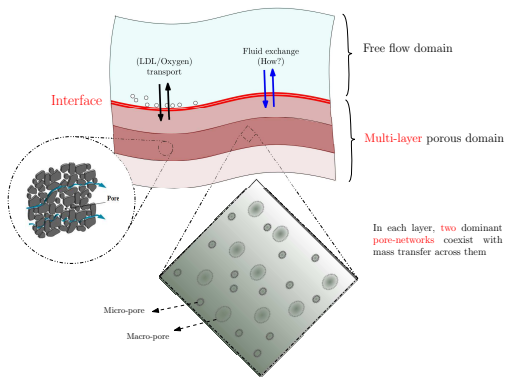
Additive manufacturing



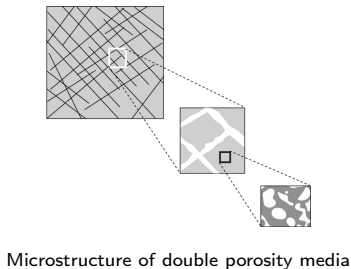
Next-generation biomedical implants

Complex physics of problem

Double porosity/permeability model



In each layer, **two dominant pore-networks** coexist with mass transfer across them



- Layered heterogeneity + coupled multi-pore networks
- system of coupled flow + transport

- What **stabilized frameworks** are available for DPP?
- When you **scaled up the size** of problem, Which FEs to use?
- How to **precondition** large system of equations arises from DPP?

What flow model governs the domain?

Double porosity/permeability model (DPP)

- Formulated flow of a fluid through a porous medium for the first time.
- Barenblatt proposed the first DPP with a simple mass transfer model between networks.



Henry Darcy (1803–1858)

Macro-pore network

Balance of Linear Momentum

$$\mu \mathbf{K}_1^{-1} \mathbf{u}_1(\mathbf{x}) + \text{grad}[p_1] = \gamma \mathbf{b}(\mathbf{x}) \quad \text{in } \Omega$$

Balance of Mass

$$\text{div}[\mathbf{u}_1] = +\chi(\mathbf{x}) \quad \text{in } \Omega$$

Boundary conditions

$$\mathbf{u}_1(\mathbf{x}) \cdot \hat{\mathbf{n}}(\mathbf{x}) = u_{n1}(\mathbf{x}) \quad \text{on } \Gamma_1^v$$

$$p_1(\mathbf{x}) = p_{01}(\mathbf{x}) \quad \text{on } \Gamma_1^p$$

Mass transfer

$$\chi(\mathbf{x}) = -\frac{\beta}{\mu}(p_1(\mathbf{x}) - p_2(\mathbf{x}))$$

Micro-pore network

Balance of Linear Momentum

$$\mu \mathbf{K}_2^{-1} \mathbf{u}_2(\mathbf{x}) + \text{grad}[p_2] = \gamma \mathbf{b}(\mathbf{x}) \quad \text{in } \Omega$$

Balance of Mass

$$\text{div}[\mathbf{u}_2] = -\chi(\mathbf{x}) \quad \text{in } \Omega$$

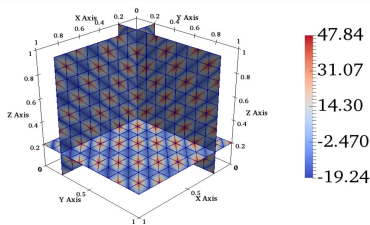
Boundary conditions

$$\mathbf{u}_2(\mathbf{x}) \cdot \hat{\mathbf{n}}(\mathbf{x}) = u_{n2}(\mathbf{x}) \quad \text{on } \Gamma_2^v$$

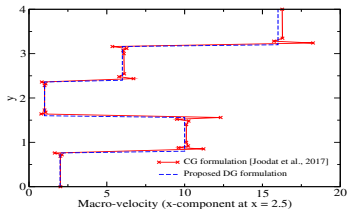
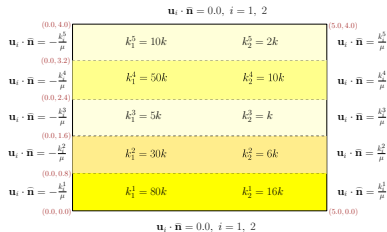
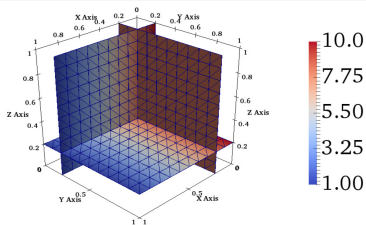
$$p_2(\mathbf{x}) = p_{02}(\mathbf{x}) \quad \text{on } \Gamma_2^p$$

Numerical hurdles

LBB violation and Gibbs phenomenon



Galerkin formulation with equal order interpolation, results in **spurious oscillations** in the pressure profile



Under the Galerkin formulation, **Gibbs phenomenon** is observed along the interfaces of the layers

Stabilized mixed DG formulation for DPP

$$\mathcal{B}_{\text{DG}}^{\text{stab}}(\mathbf{w}_1, \mathbf{w}_2, q_1, q_2; \mathbf{u}_1, \mathbf{u}_2, p_1, p_2) = \mathcal{L}_{\text{DG}}^{\text{stab}}(\mathbf{w}_1, \mathbf{w}_2, q_1, q_2)$$

The bilinear form:

$$\begin{aligned} \mathcal{B}_{\text{DG}}^{\text{stab}} := \mathcal{B}_{\text{DG}} & - \frac{1}{2} \left(\mu k_1^{-1} \mathbf{w}_1 - \text{grad}[q_1]; \mu^{-1} k_1 (\mu k_1^{-1} \mathbf{u}_1 + \text{grad}[p_1]) \right) \\ & - \frac{1}{2} \left(\mu k_2^{-1} \mathbf{w}_2 - \text{grad}[q_2]; \mu^{-1} k_2 (\mu k_2^{-1} \mathbf{u}_2 + \text{grad}[p_2]) \right) \\ & + \eta_u h \left(\{\{\mu k_1^{-1}\}\} \llbracket \mathbf{w}_1 \rrbracket; \llbracket \mathbf{u}_1 \rrbracket \right)_{\Gamma_{\text{int}}} + \eta_u h \left(\{\{\mu k_2^{-1}\}\} \llbracket \mathbf{w}_2 \rrbracket; \llbracket \mathbf{u}_2 \rrbracket \right)_{\Gamma_{\text{int}}} \\ & + \frac{\eta_p}{h} \left(\{\{\mu^{-1} k_1\}\} \llbracket q_1 \rrbracket; \llbracket p_1 \rrbracket \right)_{\Gamma_{\text{int}}} + \frac{\eta_p}{h} \left(\{\{\mu^{-1} k_2\}\} \llbracket q_2 \rrbracket; \llbracket p_2 \rrbracket \right)_{\Gamma_{\text{int}}} \end{aligned}$$

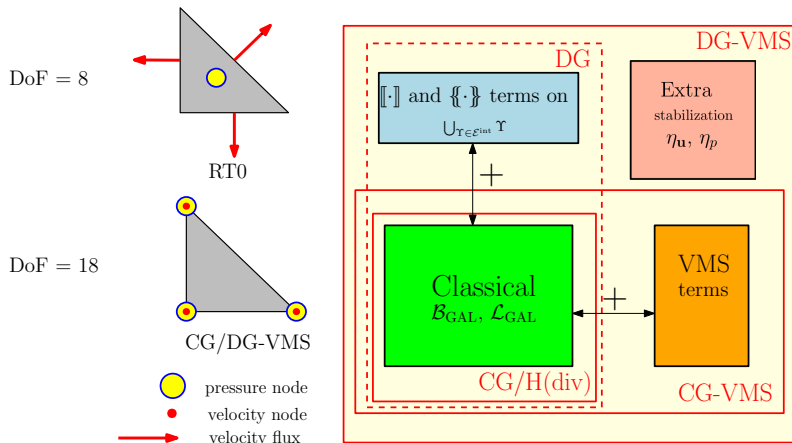
The linear functional:

$$\mathcal{L}_{\text{DG}}^{\text{stab}} := \mathcal{L}_{\text{DG}} - \frac{1}{2} \left(\mu k_1^{-1} \mathbf{w}_1 - \text{grad}[q_1]; \mu^{-1} k_1 \gamma \mathbf{b}_1 \right) - \frac{1}{2} \left(\mu k_2^{-1} \mathbf{w}_2 - \text{grad}[q_2]; \mu^{-1} k_2 \gamma \mathbf{b}_2 \right)$$

\mathcal{B}_{DG} and \mathcal{L}_{DG} : bilinear form and linear functional under conventional DG.

What are the available enriched FEs for DPP?

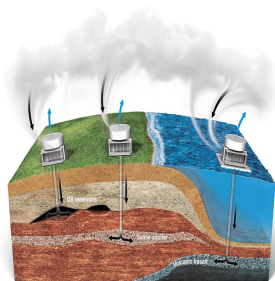
H(div) vs CG-VMS vs DG-VMS



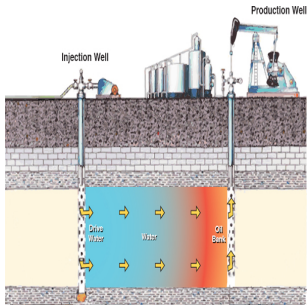
What is the best FEMs (H(div) or CG-VMS or DG-VMS) for DPP?

Real-life, large-scale problems

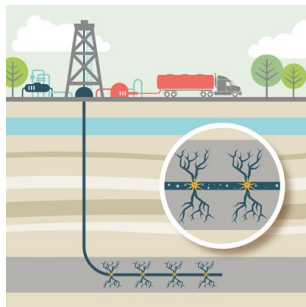
in subsurface flow and geophysical simulations



CO2 sequestration



Enhanced oil recovery



Hydraulic fracturing

- Large domains ($\sim 1\text{km} - \sim 100\text{km}$), multiscale, multiphysics couplings.
- High performance parallel processing are required for solving these problems.
- **Specialized iterative block solver methodologies are required.**

Composable block solvers I

Two approaches to effectively precondition large system of equations

Method 1: splitting by scales

$$\mathbf{K} = \begin{bmatrix} \mathbf{K}_{uu}^1 & \mathbf{K}_{up}^1 & \mathbf{0} & \mathbf{0} \\ \mathbf{K}_{pu}^1 & \mathbf{K}_{pp}^1 & \mathbf{0} & \mathbf{K}_{pp}^{12} \\ \mathbf{0} & \mathbf{0} & \mathbf{K}_{uu}^2 & \mathbf{K}_{up}^2 \\ \mathbf{0} & \mathbf{K}_{pp}^{21} & \mathbf{K}_{pu}^2 & \mathbf{K}_{pp}^2 \end{bmatrix} \begin{pmatrix} \mathbf{u}_1 \\ \mathbf{p}_1 \\ \mathbf{u}_2 \\ \mathbf{p}_2 \end{pmatrix} = \begin{pmatrix} \mathbf{f}_u^1 \\ \mathbf{f}_p^1 \\ \mathbf{f}_u^2 \\ \mathbf{f}_p^2 \end{pmatrix}$$
$$\mathbf{A} := \begin{bmatrix} \mathbf{K}_{uu}^1 & \mathbf{K}_{up}^1 \\ \mathbf{K}_{pu}^1 & \mathbf{K}_{pp}^1 \end{bmatrix}, \quad \mathbf{B} := \begin{bmatrix} \mathbf{0} & \mathbf{0} \\ \mathbf{0} & \mathbf{K}_{pp}^{12} \end{bmatrix},$$
$$\mathbf{C} := \begin{bmatrix} \mathbf{0} & \mathbf{0} \\ \mathbf{0} & \mathbf{K}_{pp}^{21} \end{bmatrix}, \quad \mathbf{D} := \begin{bmatrix} \mathbf{K}_{uu}^2 & \mathbf{K}_{up}^2 \\ \mathbf{K}_{pu}^2 & \mathbf{K}_{pp}^2 \end{bmatrix}$$

- \mathbf{A} and \mathbf{D} have similar compositions to classical mixed Poisson \rightarrow Schur complement approach.
- Individually precondition the decoupled \mathbf{A} and \mathbf{D} blocks.

$$\mathbf{A}^{-1} = \begin{bmatrix} \mathbf{I} & -(\mathbf{K}_{uu}^1)^{-1} \mathbf{K}_{up}^1 \\ \mathbf{0} & \mathbf{I} \end{bmatrix} \begin{bmatrix} (\mathbf{K}_{uu}^1)^{-1} & \mathbf{0} \\ \mathbf{0} & (\mathbf{S}^1)^{-1} \end{bmatrix} \begin{bmatrix} \mathbf{I} & \mathbf{0} \\ -\mathbf{K}_{pu}^1 (\mathbf{K}_{uu}^1)^{-1} & \mathbf{I} \end{bmatrix}$$
$$\mathbf{D}^{-1} = \begin{bmatrix} \mathbf{I} & -(\mathbf{K}_{uu}^2)^{-1} \mathbf{K}_{up}^2 \\ \mathbf{0} & \mathbf{I} \end{bmatrix} \begin{bmatrix} (\mathbf{K}_{uu}^2)^{-1} & \mathbf{0} \\ \mathbf{0} & (\mathbf{S}^2)^{-1} \end{bmatrix} \begin{bmatrix} \mathbf{I} & \mathbf{0} \\ -\mathbf{K}_{pu}^2 (\mathbf{K}_{uu}^2)^{-1} & \mathbf{I} \end{bmatrix}$$

- 1 $\mathbf{K}_{uu}^1, \mathbf{K}_{uu}^2$ are mass matrices \rightarrow $\text{ILU}(0)$ to invert.
- 2 Precondition \mathbf{S}^1 , and \mathbf{S}^2 :

$$\mathbf{S}_p^1 = \mathbf{K}_{pp}^1 - \mathbf{K}_{pu}^1 \text{diag}(\mathbf{K}_{uu}^1)^{-1} \mathbf{K}_{up}^1$$

$$\mathbf{S}_p^2 = \mathbf{K}_{pp}^2 - \mathbf{K}_{pu}^2 \text{diag}(\mathbf{K}_{uu}^2)^{-1} \mathbf{K}_{up}^2$$

- 3 Apply **multigrid V-cycle** on \mathbf{S}_p^1 and \mathbf{S}_p^2 from the HYPRE BoomerAMG.
- 4 Single sweep of flexible **GMRES** to obtain the solution of full 4×4 block system.

Composable block solvers II

Method 2: splitting by fields

$$K = \begin{bmatrix} K_{uu}^1 & 0 & K_{up}^1 & 0 \\ 0 & K_{uu}^2 & 0 & K_{up}^2 \\ K_{pu}^1 & 0 & K_{pp}^1 & K_{pp}^{12} \\ 0 & K_{pu}^2 & K_{pp}^{21} & K_{pp}^2 \end{bmatrix} \begin{pmatrix} u_1 \\ u_2 \\ p_1 \\ p_2 \end{pmatrix} = \begin{pmatrix} f_u^1 \\ f_u^2 \\ f_p^1 \\ f_p^2 \end{pmatrix}$$

$$A := \begin{bmatrix} K_{uu}^1 & 0 \\ 0 & K_{uu}^2 \end{bmatrix}, \quad B := \begin{bmatrix} K_{up}^1 & 0 \\ 0 & K_{up}^2 \end{bmatrix},$$

$$C := \begin{bmatrix} K_{pu}^1 & 0 \\ 0 & K_{pu}^2 \end{bmatrix}, \quad D := \begin{bmatrix} K_{pp}^1 & K_{pp}^{12} \\ K_{pp}^{21} & K_{pp}^2 \end{bmatrix}$$

- The inverse of K is:

$$K^{-1} = \begin{bmatrix} I & -A^{-1}B \\ 0 & I \end{bmatrix} \begin{bmatrix} A^{-1} & 0 \\ 0 & S^{-1} \end{bmatrix} \begin{bmatrix} I & 0 \\ -CA^{-1} & I \end{bmatrix}.$$

- A is mass matrix \rightarrow use $ILU(0)$.
- Precondition S^{-1} by employing diagonal mass-lumping of A :

$$S_p = D - C \text{diag}(A)^{-1} B$$

$$= \begin{bmatrix} K_{pp}^1 - K_{pu}^1 \text{diag}(K_{uu}^1) K_{up}^1 & & & \\ & K_{pp}^{12} & & \\ & & K_{pp}^2 - K_{pu}^2 \text{diag}(K_{uu}^2) K_{up}^2 & \\ & & & \end{bmatrix}$$

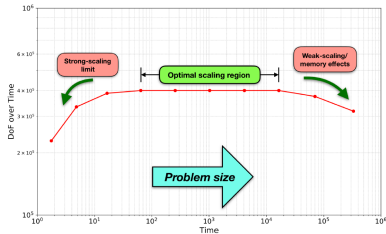
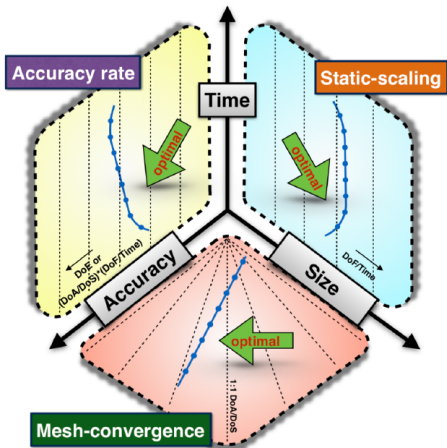
- Apply V -cycle on each diagonal block.
- Single sweep of flexible $GMRES$ to obtain the solution of full system.

Which method performs better?

How to gauge parallel performance and scalability?

Performance spectrum modeling

(Time-Accuracy-Size) TAS model



METRICS:

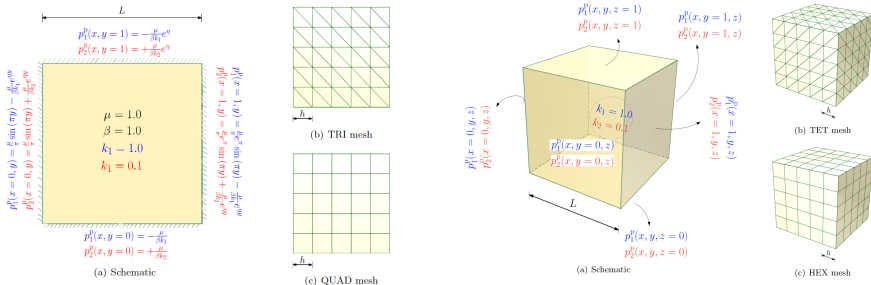
- Parallel efficiency = $\frac{Time_1}{Time_p \times \# \text{ MPI processors}} \%$
- Digits of Accuracy DoA: $= -\log_{10}(L_2^{\text{norm}})$
Digits of Size DoS: $= -\log_{10}(DoF)$
- Digits of Efficacy DoE: $= -\log_{10}(L_2^{\text{norm}} \times Time)$

Numerical results

2D/3D DPP problems with analytical solution

We used the composable solvers feature in *PETSc* and the FE libraries under the *Firedrake Project*.

Method of manufactured solutions:



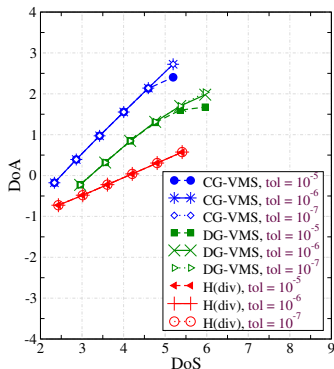
What is the best FEMs (H(div) or CG-VMS or DG-VMS)?

We use TAS model

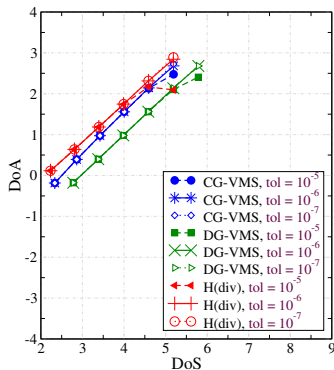
FEs comparison (mesh convergence)

Macro-velocity field

TRI mesh



QUAD mesh

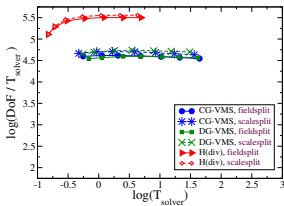
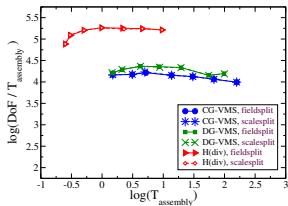
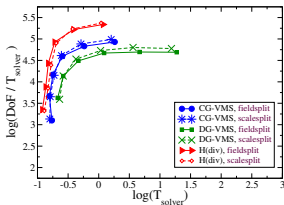
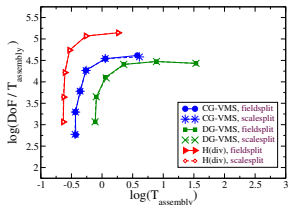


- VMS slope ≈ 1 . H(div) slope ≈ 0.5
- Numerical accuracy: VMS $>$ H(div)
- Tight solver tol is needed to avoid flattening out.
- Same pattern observed for \mathbf{u}_2, p_1 , and p_2 .

- VMS slope ≈ 1 .
- H(div) shows super. conv. close ≈ 1 .
- Numerical accuracy: VMS \gtrsim H(div).

FEs comparisons (static scaling results)

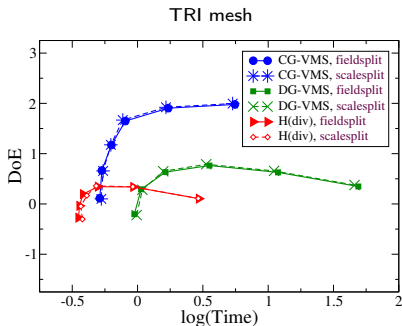
2D vs 3D for simplicial elements



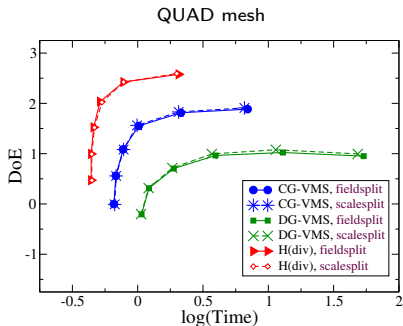
- H(div) formulation processes its DoF count faster than either of the VMS formulations.
- Assembly algorithm in 2D vs 3D

FEs comparisons (Digits of Efficacy)

Macro velocity



● DoE: CG-VMS \gg DG-VMS > H(div).



● DoE: H(div) > CG-VMS > DG-VMS.

Solver strategies comparisons (Strong-scaling @ 200K DoF)

Field-splitting

Scale-splitting

No. of MPI proc.	TET mesh					TET mesh				
	Time			KSP	Parallel eff. (%)	Time			KSP	Parallel eff. (%)
	Assembly	Solver	Total			Assembly	Solver	Total		
1	9.11E-01	6.62E-01	1.57E+00	15	100	9.14E-01	6.19E-01	1.53E+00	15	100
2	6.25E-01	5.20E-01	1.15E+00	16	68.7336	6.07E-01	4.92E-01	1.10E+00	16	69.8543
4	4.10E-01	3.51E-01	7.60E-01	16	51.7627	4.25E-01	3.36E-01	7.61E-01	16	50.4008
8	3.63E-01	2.70E-01	6.33E-01	16	31.092	3.81E-01	2.83E-01	6.63E-01	16	28.9085
12	3.87E-01	3.04E-01	6.90E-01	16	18.9986	3.36E-01	2.68E-01	6.04E-01	16	21.168
16	3.63E-01	3.00E-01	6.62E-01	16	14.8513	3.82E-01	2.73E-01	6.55E-01	16	14.6352

No. of MPI proc.	TET mesh					TET mesh				
	Time			KSP	Parallel eff. (%)	Time			KSP	Parallel eff. (%)
	Assembly	Solver	Total			Assembly	Solver	Total		
1	1.23E+01	5.01E+00	1.73E+01	13	100	1.25E+01	4.14E+00	1.66E+01	13	100
2	7.95E+00	3.39E+00	1.13E+01	15	76.455	7.84E+00	2.80E+00	1.06E+01	15	77.9605
4	4.81E+00	1.99E+00	6.80E+00	15	63.7406	4.84E+00	1.64E+00	6.48E+00	15	64.0244
8	3.16E+00	1.26E+00	4.42E+00	16	49.0052	3.32E+00	1.11E+00	4.43E+00	16	46.8009
12	2.99E+00	1.06E+00	4.05E+00	16	35.6702	2.90E+00	9.59E-01	3.86E+00	16	35.8439
16	2.42E+00	9.54E-01	3.38E+00	16	32.1111	2.44E+00	8.38E-01	3.28E+00	16	31.6313

No. of MPI proc.	TET mesh					TET mesh				
	Time			KSP	Parallel eff. (%)	Time			KSP	Parallel eff. (%)
	Assembly	Solver	Total			Assembly	Solver	Total		
1	8.08E+00	5.40E+00	1.35E+01	19	100	7.81E+00	4.11E+00	1.19E+01	19	100
2	4.76E+00	8.27E+00	1.30E+01	79	51.7268	4.57E+00	6.62E+00	1.12E+01	79	53.2618
4	2.55E+00	5.45E+00	7.99E+00	102	42.1566	2.54E+00	4.43E+00	6.97E+00	102	42.7301
8	1.91E+00	3.37E+00	5.27E+00	109	31.9492	1.85E+00	2.88E+00	4.73E+00	109	31.5077
12	1.98E+00	2.69E+00	4.67E+00	111	24.0646	1.88E+00	2.36E+00	4.24E+00	111	23.4498
16	1.61E+00	2.52E+00	4.13E+00	119	20.4045	1.61E+00	2.26E+00	3.87E+00	119	19.2556

H(div)

CG-VMS

DG-VMS

- Scale-splitting methodology **slightly more efficient** in terms of time-to-solution.
- Both methods have **same KSP counts**.

Concluding remarks:

- Proposed a framework for performance analysis of various “enriched FEs” for the DPP model.
- The **VMS** formulations yield much **higher overall numerical accuracy** for all velocity and pressure fields.
- **Type of mesh** (simplicial or non-simplicial) affects the digits of efficacy.
- Regardless of mesh type, **DoFs are processed the fastest under the H(div) formulation** compared to other formulations.
- **Both** composable solvers are **scalable** in both parallel and algorithmic senses.
- Both solvers exert similar overall effects on performance metrics.

-  M. S. Joshaghani, J. Chang, K. B. Nakshatrala, and M. G. Knepley, “*On composable block solvers and performance spectrum analysis for double porosity/permeability model*,” **Journal of Computational Physics**, 2019.
-  M. S. Joshaghani, S. H. Joodat, and K. B. Nakshatrala, “*A stabilized mixed discontinuous Galerkin formulation for double porosity/permeability model*,” Tentatively accepted in **Computer Methods in Applied Mechanics and Engineering**, 2019.

Thank you

Contact

Mohammad S. Joshaghani (msarra@joshaghani@uh.edu)

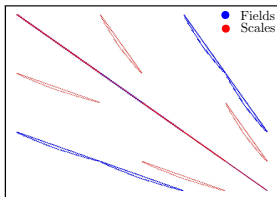
Kalyana B. Nakshatrala (knakshatrala@uh.edu)

Computational & Applied Mechanics Laboratory
Department of Civil & Environmental Engineering
University of Houston, Houston, Texas.

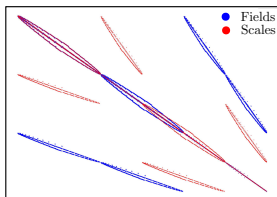
Field-splitting vs Scale-splitting

Global matrix with DoF=1k

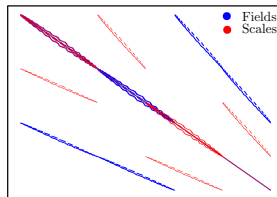
CG-VMS



DG-VMS



H(div)



- Smaller bandwidth in scale-split method → better performance wrt time.
- The **sparsity pattern** of the subblocks → the **performance differences** of solvers.